

## Estimating shear-waves velocity structure by using array methods (FK and SPAC) and inversion of ellipticity curves at a site in south of Tehran

E. Shabani<sup>1</sup>, C. Cornou<sup>2</sup>, E. Haghshenas<sup>3</sup>, M. Wathelet<sup>2</sup>, P.-Y. Bard<sup>2</sup>, N. Mirzaei<sup>1</sup>, and M. Eskandari-Ghadi<sup>4</sup>

<sup>1</sup> *Institute of Geophysics, University of Tehran, Iran,*

<sup>2</sup> *Laboratoire de Géophysique Interne et Tectonophysique, Université J. Fourier, IRD, LCPC, CNRS, Maison des Géosciences, BP53, 38041 Grenoble cedex 9, France,*

<sup>3</sup> *International Institute of Earthquake Engineering and Seismology, Tehran, Iran*

<sup>4</sup> *Dep. of Eng. Science, University of Tehran, Tehran, Iran.*

*Email: eshabani@ut.ac.ir, Cecile.Cornou@obs.ujf-grenoble.fr, haghshen@iiees.ac.ir, marc@geopsy.org, bard@obs.ujf-grenoble.fr, nmirzaii@ut.ac.ir, ghadi@ustmb.ac.ir*

### ABSTRACT :

Tehran, capital of Iran, is under the threat of large magnitude earthquakes (above 7) located on very near faults. Previous studies on the effect of local surface geology on earthquake ground motion by using 1D calculation of SH transfer function (Jafari et al, 2001; JICA & CEST, 2000) and by using experimental methods (Haghshenas, 2005) based on earthquake and ambient noise vibration recordings resulted in very different and unexpected results. By assuming a layer with  $V_s = 700$  m/s as seismic bedrock, 1D SH transfer functions show indeed a weak amplification for frequencies above 2 Hz, while the site-to-reference spectral ratios exhibit a significant amplification (up to 8) within a large frequency band from 0.3 to 8 Hz. Such discrepancy might be explained by very thick and stiff sedimentary layers overlaying very rigid bedrock. In order to better constrain shear-wave velocities at depth, we thus derived dispersion curves of Rayleigh waves by using SPAC and FK array methods and extracted Rayleigh waves ellipticity curves by using a recently proposed method based on the wavelet decomposition of the noise wave field. Dispersion and ellipticity curves are then simultaneously inverted to get the shear wave velocities. In this paper, we show results obtained at a site in the southern part of the city that exhibit rather stiff sedimentary  $V_s$  structure overlaying a bedrock whose depth is within 700 and 1200 meters.

### KEYWORDS:

shear-waves velocity structure, ambient noise array techniques, Rayleigh waves, ellipticity curves, Tehran

## 1. INTRODUCTION

While seismic scenarios performed in Tehran predicted small to moderate amplification throughout the city at frequencies higher than 2 Hz (Jafari et al, 2001; JICA & CEST, 2000), seismological experiments have shown very large ground motion amplification over a wide frequency range (from 0.3 to 8 Hz) (Haghshenas, 2005). Seismic scenarios being derived by considering site amplification due to unconsolidated superficial layers having shear velocity lower than 700 m/s only, such discrepancy might be explained by very thick and stiff sedimentary layers overlaying very rigid bedrock. Use of ambient noise recordings (array and single-station methods) is a powerful tool to determine site response properties, especially for deep sedimentary structure. In this paper, we have thus used these techniques to constrain shear-wave velocities over a large depth range at a site located in southern Tehran, which shows the most important site amplification (Haghshenas, 2005).

First, we measured dispersion curves of Rayleigh waves from ambient array noise data recorded at two nearby sites in southern Tehran located nearby a 150 meters deep borehole. Due to limited aperture of the array, only the highest frequency part of the dispersion curve could be measured. In order to retrieve information on the dispersive characteristics of Rayleigh waves at lower frequencies, we then extracted Rayleigh waves ellipticity curves by using 24 hours noise recordings. Finally dispersion and ellipticity curves are jointly inverted in order to derive shear-wave velocity profiles over a large depth range. Bedrock depth is then determined by comparing resonance frequency provided by SH transfer functions computed on inverted Vs profiles and the actual resonance frequency.

## 2. ARRAY AND SINGLE STATIONS MEASUREMENTS

Figure 1 shows location of the 14 single-station sites investigated by Haghshenas (2005) and the two ambient noise array measurements performed in 2007. Single-station noise measurements were performed for 5 months in 2002 by using CMG40 sensors. The array measurements were conducted by using two circular arrays of 8 stations each equipped with Guralp CMG6TD seismic stations (Figure 2). Maximum aperture of these two arrays was 100 m (array A) and 50 m (array B). These arrays are located nearby a 150 meters deep borehole site and nearby MOF site which is a low resonance frequency site (resonance frequency around 0.3-0.4 Hz) exhibiting the largest ground motion amplification (Haghshenas (2005).

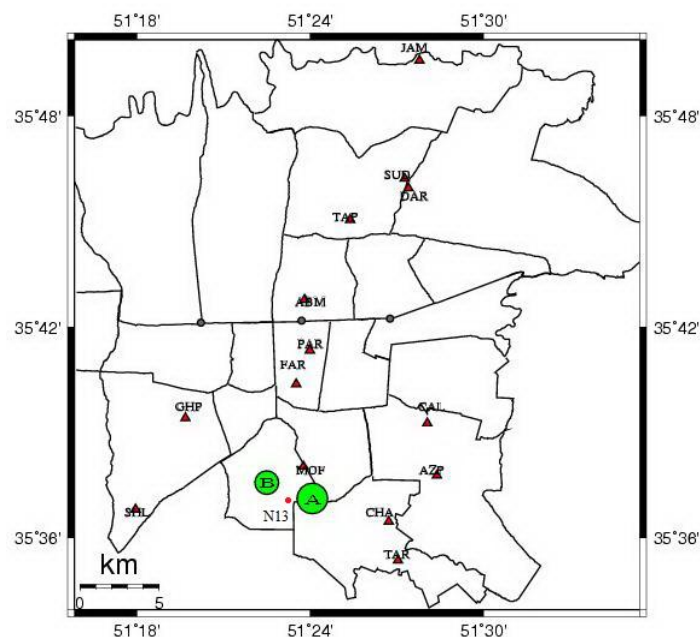


Figure 1 Location of 14 single stations (triangles), two array measurements A and B and the nearest borehole (N13) to the MOF station on the Tehran map.

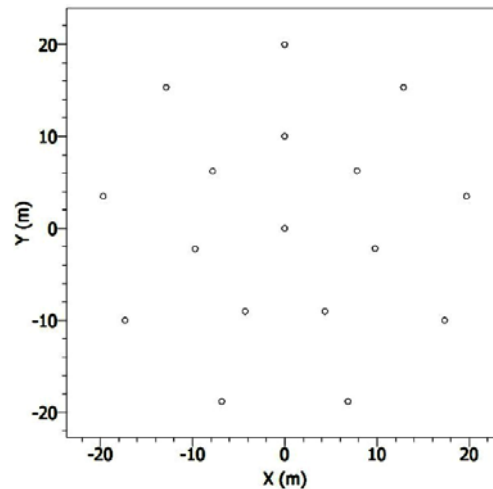


Figure 2 Array layout for array B composed of two nested circular arrays composed of 8 stations each (including the central station).

### 2.1. Array Methods

The SPAC method was first introduced by Aki (1957) to reveal the nature of the background seismic noise and also the wave propagation characteristics. The SPAC method is designed to estimate the dispersion curves for surface waves by analyzing the correlation between noise recordings made at nearby sites. From these curves, we can characterize the structure of the underlying propagation medium. Since the method is based on a statistical investigation in time and space, we assume that the signal is a stochastic noise, stationary in both domains (Bettig et al., 2001). Frequency-wave number (F-K, Lacoss et al. 1969, Kvaerna and Ringdahl 1986) analysis assumes horizontal plane waves traveling across the array of sensors. Considering a wave with frequency  $f$ , a direction of propagation and a velocity (or equivalently  $k_x$  and  $k_y$ , wavenumbers along X and Y horizontal axis, respectively) the relative arrival times are calculated at all sensor locations and the phases are shifted according to the time delays. The array output is calculated by the summation of shifted signals in the frequency domain. If the waves effectively travel with the given direction and velocity, all contributions will stack constructively, resulting in a high array output. The array output divided by the spectral power is called the semblance (Lacoss et al. 1969, Asten and Henstridge, 1984). The location of the maximum of semblance in the plane  $(k_x, k_y)$  provides an estimate of the velocity and of the azimuth of the traveling waves across the array.

In this study, array processing by using MSPAC (Bettig et al., 2001) and FK techniques was performed by using Sesarray software package (<http://www.geopsy.org>; Wathelet et al., 2008). Figure 3b shows measured dispersion curves by FK analysis (back dots). Results from MSPAC analysis are not shown here since it did not add more significant results to the dispersion curve than the one derived from FK analysis. Inversion was performed by using the Conditional Neighborhood Algorithm (Wathelet, 2008). Inversion of dispersion curves being non-unique, Figure 3a shows the ensemble of inverted shear-wave profiles that explain in a similar way the observed phase velocities (Figure 3b). Although inverted shear wave velocity profiles fit well the borehole  $V_s$  measurements (Figure 3a, black line), they do not provide any constrain of  $V_s$  for depths deeper than 100 meters. This is explained by the limited array aperture resulting to phase velocity estimates ranging between 6 and 10 Hz.

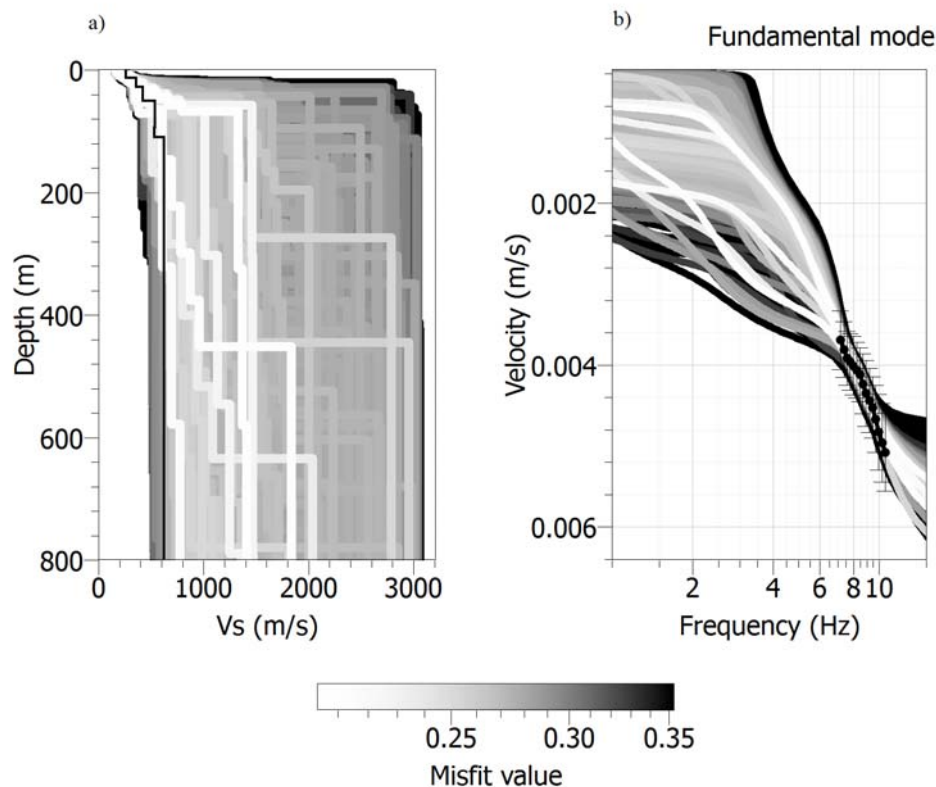


Figure 3 Inversion results at array B. (a) Inverted shear-wave profiles overlaid by the thin black line corresponding to the shear-wave profile derived from borehole measurements (the borehole depth is 120m), (b) Dispersion curves corresponding to inverted Vs and the observed dispersion curve including standard deviation (black dots). The scale corresponds to the misfit values as defined in Wathelet (2008).

## 2.2. Extraction of ellipticity curves and joint Inversion of Dispersion-Ellipticity Curves

In order to extract information on the dispersive characteristics of Rayleigh waves at frequencies lower than 6 Hz which will add information on the velocity structure at larger depths, we extracted ellipticity curves of Rayleigh waves by using 24 hours of microtremors recorded at MOF station by Haghshenas (2002). The method used is based on an algorithm proposed by Fäh et al. (2001, 2003) that allows locating P-SV wavelets in the time-series through frequency-time analysis (TFA). This method allows indeed minimizing the effects of contribution of SH waves and the effects of the superposition of different incoming P-SV waves in the calculated H/V ratios. Velocity structure within sediments is mostly controlled by the right flank of the ellipticity curve ranging from the ellipticity peak frequency to the frequency of the first minimum. At MOF site, extracted ellipticities are shown in Figure 4b (black dots). Ellipticity and dispersion curves are then jointly inverted by using the inversion algorithm of Wathelet (2008). Inverted Vs profiles are shown in Figure 4c. Extracted ellipticities providing information within the frequency band from 0.5 to 0.8 Hz, shear-wave velocities are better constrained over larger depths than by using inversion of dispersion curve alone (Figure 3b). However, even though such joint inversion provides the general shape of shear-wave velocity structure within sediments, bedrock depth is not constrained.

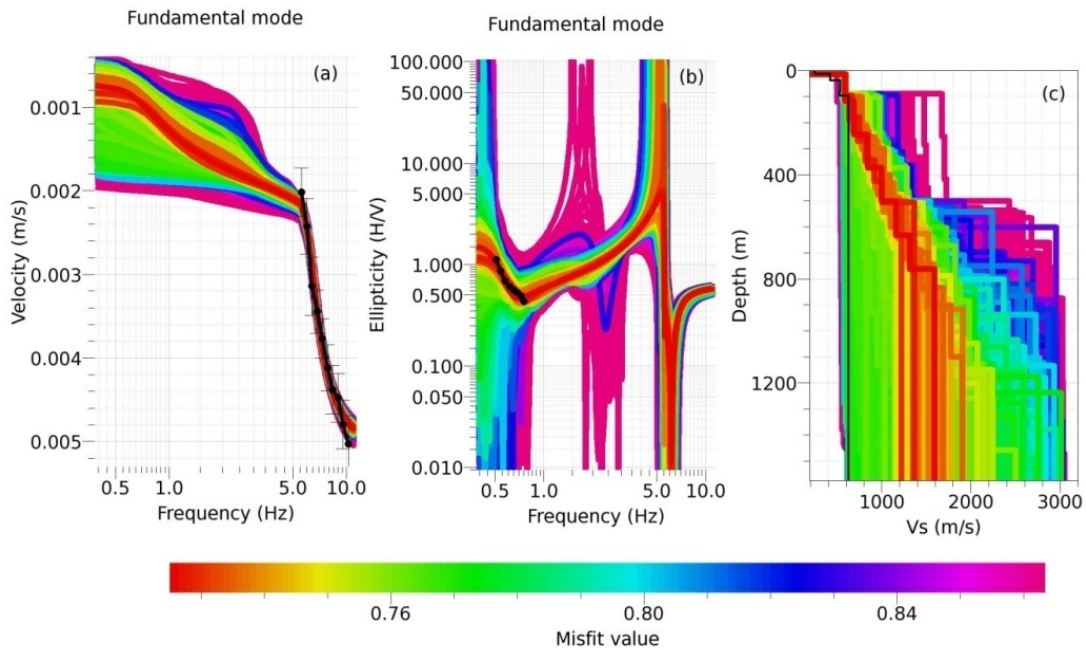


Figure 4 Joint Inversion of FK dispersion curve analysis and the ellipticity of array B.

### 3. DERIVATION OF BEDROCK DEPTH

In order to constrain the bedrock depth, one may also introduce resonance frequency in the joint inversion procedure. We have observed however that inverted profiles are very sensitive to the weight on different input data (dispersion curves, ellipticity curves and resonance frequency) introduced during the inversion for computing the global misfit function. We also prefer to compute the SH transfer functions for the ensemble of inverted Vs profiles and by scanning different bedrock depths. Here, we simply considered bedrock depths varying from 400 to 1400 meters with a bedrock depth step of 100 m and fixed the bedrock velocity to 5600 m/s and 3200 m/s for P- and S-waves velocities, respectively. Then, for these different scenarios of bedrock depth, resonance frequencies provided by the SH transfer functions are compared to the actual resonance frequency derived by Haghshenas (2002) in order to find out the range of bedrock depth that can best satisfy the known fundamental resonance frequency. At MOF site, previous studies performed by Haghshenas (2005) found the fundamental resonance frequency between 0.4 to 0.5 Hz using site-to-reference method and between 0.27 and 0.4 Hz using microtremors (H/V) (Figure 5). For comparison with SH transfer function, we consider here that the resonance frequency is in-between 0.27 and 0.5 Hz.

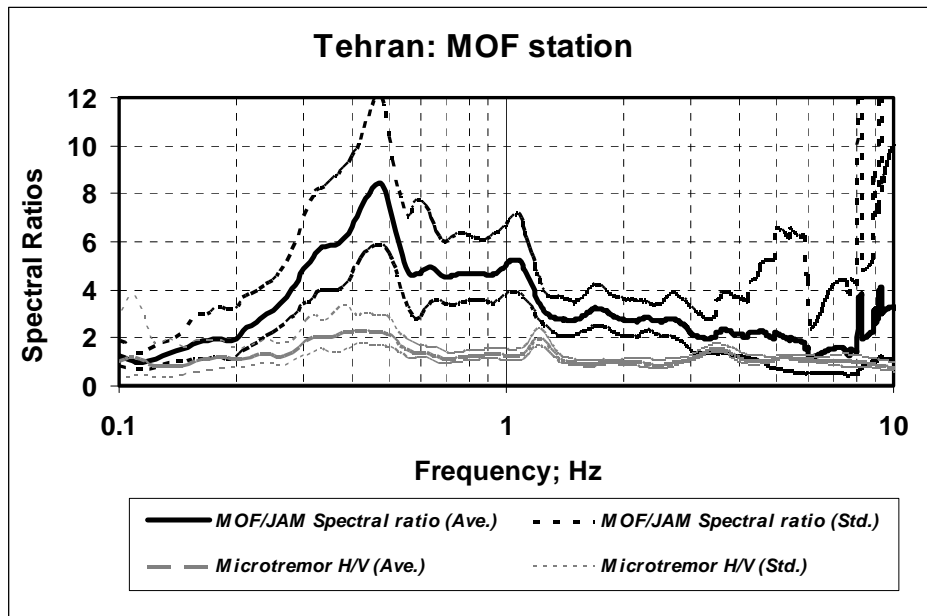


Figure 5 Comparison of the average spectral ratios calculated by two different methods at MOF stations: Site to Reference method (black lines) and Microtremor H/V (gray lines), the reference site (JAM) is on rock and locates in the north of Tehran (Haghshenas, 2005)

Here, we selected the shear velocity models having misfit less than 0.76 for calculation of SH transfer function (Figure 4c). Example of SH transfer functions computed by fixing the bedrock depth at 1000m is presented in Figure 6. In this figure, transfer functions show fundamental resonance frequencies between 0.35 to 0.39 Hz that is in agreement with the known resonance frequency. After scanning different bedrock depth, we found out that the bedrock depth should lie between 700 and 1200 meters in this part of Tehran.

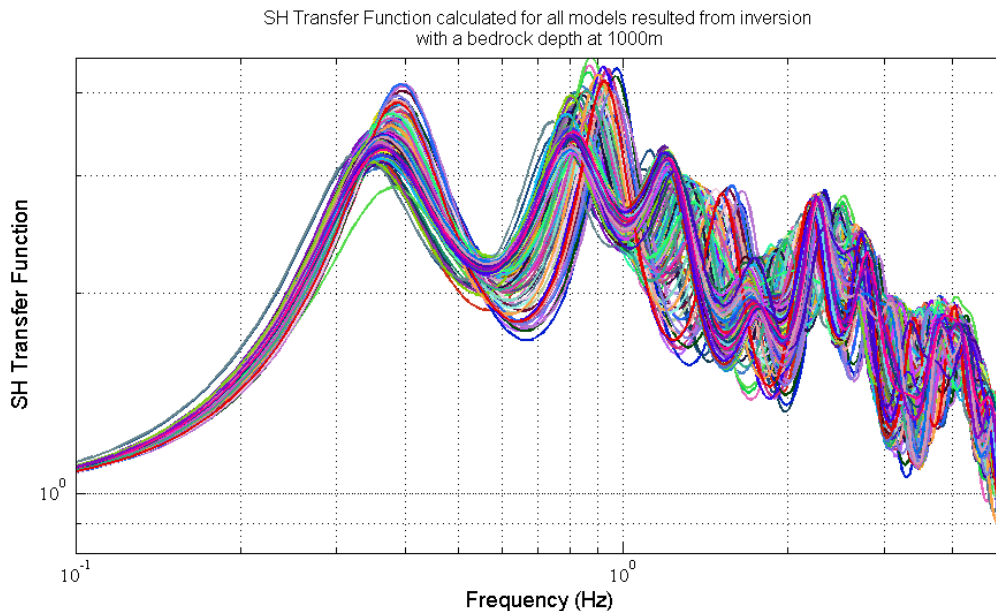


Figure 6 SH transfer function calculated for all inverted Vs profile having misfit lower than 0.76 (see Figure 4) and by fixing a bedrock depth at 1000m.

#### 4. CONCLUSION

Different methods including microtremors array (FK and SPAC), H/V calculated by TFA techniques, joint inversion of dispersion curves and ellipticity curves and finally SH transfer function were used to constrain the shear-wave velocity and the bedrock depth at a site exhibiting high ground motion amplification at low frequency in south of Tehran. Results show that using the array data alone (arrays with a limited aperture of 100 meters) can only provide  $V_s$  profile for the superficial layers. Combining the array methods and single station measurement can give deeper and better constrain on shear-wave velocity models. Knowing the range of fundamental resonance frequencies from earthquake data give us the opportunity to filter the inverted  $V_s$  models obtained from joint inversion of dispersion curve and H/V ellipticity curve, by applying SH transfer functions calculated for various inverted  $V_s$  profile and comparing subsequent resonance frequency to the actual one. Applying this procedure give us an idea about the shear-wave velocity and the bedrock depth in south of Tehran which may lie between 700 to 1200 meters. This procedure should be applied to different sites in Tehran in order to retrieve the  $V_s$  profile and the spatial variation of sediment-to-bedrock depth throughout Tehran. This will then allow to better understand observed site amplification.

#### REFERENCES

- Aki, K. (1957). Space and time spectra of stationary stochastic waves, with special reference to microtremors, *Bull. Earthq. Res. Inst.* 35, 415-456.
- Bettig, B., P.-Y. Bard, F. Scherbaum, J. Riepl, F. Cotton, C. Cornou and D. Hatzfeld (2001). Analysis of dense array noise measurements using the modified spatial auto-correlation method (SPAC). Application to the Grenoble area., *Bolletino di Geosica Teorica ed Applicata* 42, 281-304.
- Kvaerna, T. and F. Ringdahl (1986). Stability of various fk-estimation techniques, in *Semiannual Technical Summary*, 1 October 1985 - 31 March 1986, In *NORSAR Scienti\_c Report*, 1-86/87, Kjeller, Norway, 29-40.
- Lacoss, R. T., E. J. Kelly and M. N. Toksoz (1969). Estimation of seismic noise structure using arrays, *Geophysics* 34, 21-38.
- Fäh, D., Kind, F. and Giardini, D. (2001). A theoretical investigation of average H/V ratios, *Geophys. J. Int.* 145, 535-549.
- Fäh, D., Kind, F. and Giardini, D. (2003). Inversion of local S-wave velocity structures from average H/V ratios, and their use for the estimation of site-effects. *Journal of Seismology* 7, 449-467.
- Haghshenas E., Bard, P.-Y., Jafari, M. K. and Hatzfeld, D. (2003). Effets de site et risque sismique à Téhéran : Premiers résultats d'une étude expérimentale. 6ème colloque national AFPS, 2003, Paris France.
- Haghshenas E. (2005). Condition Géotechniques et Aléa Sismique Local à Téhéran ; Ph.D Thesis of the Joseph Fourier University, Grenoble, France.
- Jafari ,M.K., Razmkhah, A., Keshavarz-Bakhshayesh, M., Sohrabi, A., and Pourazin Kh. (2001). Etude Complémentaire de Microzonage Sismique au Sud de Téhéran. *IIEES, Spec. Pub. (In persan)*.
- JICA (Japan International Cooperation Agency) & CEST (Centre for Earthquake & Environmental Studies of Tehran, Tehran Municipality), (2000). *The Study on Seismic Microzoning of the Greater Tehran Area in The Islamic Republic of Iran, Final report*.
- Wathelet, M. (2008). An improved neighborhood algorithm: parameter conditions and dynamic scaling. *Geophysical Research Letters*, 35, L09301, doi:10.1029/2008GL033256.
- Wathelet, M., D. Jongmans, M. Ohrnberger, and S. Bonnefoy-Claudet (2008). Array performances for ambient vibrations on a shallow structure and consequences over  $V_s$  inversion. *Journal of Seismology*, 12, 1-19.